X-Ray Dynamical Diffraction Process Inside a Distorted Crystal

S. Takagi

Department of Physics, Faculty of Science and Technology Science, University of Tokyo, Noda, Japan

Z. Naturforsch. **37a**, 460–464 (1982); received February 9, 1982

Dedicated to Prof. G. Hildebrandt on the occasion of his 60th birthday

It is shown that the dynamical diffraction process inside a distorted crystal consists of ordinary dynamical progression inside perfect portions of the crystal and scattering at distortions. The scattered waves proceed as in the perfect crystal and can be multiply scattered. The sum of the primary wave induced at the entrance surface and the waves scattered at distorted parts inside the "inverted Borrmann triangle" gives the resultant wave field at the exit surface.

Introduction

The dynamical diffraction process inside a distorted as well as a perfect crystal can be described by a set of partial differential equations developed by the present author [1], [2]. Several methods for solving these equations have been developed [2] to [7]. For distorted crystals, the direct numerical integration may be the most convenient one and has been widely used to simulate the contrast of X-ray diffraction topographs of various kinds of defects inside a nearly perfect crystal. In this method one has only to introduce the strain distribution inside the crystal and the boundary conditions comprising the condition of incidence and one gets the simulation of the image, but one cannot get any information about what is happening inside the crystal. The crystal is a kind of black box.

A perturbation approach, i.e. the solution by successive approximation to the equivalent integral equations has been developed [8], [9]. This method provides an explanation of the diffraction process by the scattering at defects and the ordinary dynamical progression inside perfect portions of the crystal. A brief decription of this method will be given here.

Theoretical Development

Incident X-rays of the wave number K fall upon a nearly perfect crystal satisfying closely or exactly the Bragg condition concerning a set of lattice planes with the reciprocal lattice vector $\boldsymbol{h}$. The wave function $\psi(\boldsymbol{r})$, which represents the magnitude of electric displacement $\boldsymbol{D}$ due to the X-ray wave in the crystal, can be expressed as

$$\psi(\boldsymbol{r}) = \psi_0(\boldsymbol{r}) \exp(-2\pi i \boldsymbol{k}_0 \cdot \boldsymbol{r}) + \psi_h(\boldsymbol{r}) \exp(-2\pi i \boldsymbol{k}_h \cdot \boldsymbol{r}), \quad (1)$$

where the first term on the right-hand side represents the incident wave in the crystal and the second the Bragg-reflected wave, $\boldsymbol{k}_0$ and $\boldsymbol{k}_h$ being their wave vectors connected by

$$\boldsymbol{k}_h = \boldsymbol{k}_0 + \boldsymbol{h}, \quad (2)$$

and $\psi_0(\boldsymbol{r})$, $\psi_h(\boldsymbol{r})$ their complex amplitudes which are slowly varying functions of position expressing all the variations of the two waves. In the Ewald-Laue theory variation of each of these two waves are given by a sum of two Bloch waves which are the functions of type (1) with constant amplitudes ψ_0 and ψ_h. The superposition of two Bloch waves with slightly different wave vectors $\boldsymbol{k}_0$ gives rise to amplitude modulation of both incident and diffracted waves known as Pendellösung effect. In distorted crystals, however, the modulation of the amplitudes is much more complicated and the wave in the crystal is expressed by a single function (1) with slowly varying amplitudes $\psi_0(\boldsymbol{r})$ and $\psi_h(\boldsymbol{r})$.

The differential equations governing the variation of $\psi_0(\boldsymbol{r})$ and $\psi_h(\boldsymbol{r})$ have been obtained in [1], [2]. They are written as

$$\frac{\partial \psi_0}{\partial s_0'} = -i\pi K C \chi'_{-h} \psi_h,$$

$$\frac{\partial \psi_h}{\partial s_h} = -i\pi K C \chi'_h \psi_0 + i 2\pi K_{\beta_h} \psi_h \quad (3)$$

Reprint requests to Dr. S. Takagi, Department of Physics, Faculty of Science and Technology, Science University of Tokyo, Noda, 278/Japan.

0340-4811 / 82 / 0500-0460 $ 01.30/0. — Please order a reprint rather than making your own copy.

(Eqs. (42) of Ref. [2]). Here s_0 and s_h are the oblique coordinates parallel to $\boldsymbol{k}_0$ and $\boldsymbol{k}_h$, respectively, C is the polarization factor and β_h the parameter describing the variation from the Bragg condition given by

$$\beta_h = (|\boldsymbol{k}_h| - k)/K .$$

where k is the mean wave number in the crystal. χ_h' is given by

$$\chi_h' = \chi_h \exp(2\pi i(\boldsymbol{h}\cdot\boldsymbol{u})), \tag{4}$$

where $\boldsymbol{u}(\boldsymbol{r})$ is the displacement of the atom at the position $\boldsymbol{r}$, and χ_h the Fourier coefficient of $\chi(\boldsymbol{r})$. The polarizability of the crystal is given by

$$\chi(\boldsymbol{r}) = -\frac{e^2\lambda^2}{\pi m c^2} n(\boldsymbol{r}), \tag{5}$$

$n(\boldsymbol{r})$ being the electron density at $\boldsymbol{r}$, other notations having their usual meaning. It must be emphasized here that $\boldsymbol{h}$ in (2) is not the "local reciprocal lattice vector",

$$\boldsymbol{h}' = \boldsymbol{h} - \frac{\partial}{\partial s_h}(\boldsymbol{h}\cdot\boldsymbol{u}),$$

on which most of the theoretical treatment of [2] was based, but it is in fact the reciprocal lattice vector of the perfect part of the crystal being considered as constant all over the crystal. In (3) the coefficients χ'_{-h} and χ'_h are functions of position and β_h is constant. In a similar set of equations ((40) of Ref. [2]) χ'_{-h} and χ'_h are replaced by χ_{-h} and χ_h (constants) and β_h by β_h' (a function of position). Hereafter the wave vector k_0 is taken as satisfying the Bragg condition exactly so that the value of β_h is always zero, $\boldsymbol{k}_h$ satisfying (2). This can be done since the effect caused by adoption of different $\boldsymbol{k}_0$ and $\boldsymbol{k}_h$ can be compensated by proper choice of the functions $\psi_0(\boldsymbol{r})$ and $\psi_h(\boldsymbol{r})$.

Differentiation of the first of the Eq. (3) with $\beta_h = 0$ with respect to s_h and utilization of both of (3) gives

$$\frac{\partial^2\psi_0}{\partial s_0\,\partial s_h}(s_0, s_h) + \pi^2 K^2 C^2 \chi_{-h}\chi_h \psi_0(s_0, s_h) = -i\pi K C \chi_{-h}\frac{\partial}{\partial s_h} \cdot \exp(-i2\pi\boldsymbol{h}\cdot\boldsymbol{u}(s_0, s_h))\,\psi_h(s_0, s_h). \tag{6}$$

Application of Riemann's method to (6), the right-hand side being considered as a function of s_0 and s_h, gives

$$\psi_0(s_0, s_h) = \psi^0_{(0)}(s_0, s_h) + \iint_{\nabla} \frac{\partial}{\partial s_h'} \cdot \exp(-i2\pi\boldsymbol{h}\cdot\boldsymbol{u}(s_0, s_h)) \cdot [-i\pi K C \chi_{-h} v(s_0, s_h; s_0', s_h')] \cdot \psi_h(s_0', s_h')\frac{dV'}{\sin 2\theta}, \tag{7}$$

where $\psi_0^{(0)}(s_0, s_h)$ is the solution for a perfect crystal, given by

$$\psi_0^{(0)}(s_0, s_h) = \Phi_0(s_0, s_h) - \int_B^A \frac{\partial}{\partial s_h'} v(s_0, s_h; s_0', s_h') \cdot \Phi_0(s_0', s_h')\frac{\gamma_0(\xi)}{\sin 2\theta_B} d\xi . \tag{8}$$

Here $\Phi_0(s_0, s_h)$ is the complex amplitude of the incident wave, which is expressed as

$$\Psi(\boldsymbol{r}) = \Phi_0(\boldsymbol{r})\exp(-i2\pi\boldsymbol{k}_0\cdot\boldsymbol{r}), \tag{9}$$

$\boldsymbol{k}_0$ being the wave vector in the crystal appearing in (2), instead of the usual expression

$$\Psi(\boldsymbol{r}) = \Psi_0(\boldsymbol{r})\exp(-i2\pi\boldsymbol{K}\cdot\boldsymbol{r})$$

with the wave vector in vacuum, $\boldsymbol{K}$, so that

$$\Phi_0(\boldsymbol{r}) = \Psi_0(\boldsymbol{r})\exp(-i2\pi[\boldsymbol{K} - \boldsymbol{k}_0]\cdot\boldsymbol{r}).$$

The double integral in (7) is over the inverted Borrmann triangle PAB shown in Fig. 1,

$$dV' = \sin 2\theta_B \cdot ds_0'\, ds_h'$$

being the surface element in (s_0', s_h') space. The single integral in (8) is over the portion BA of the

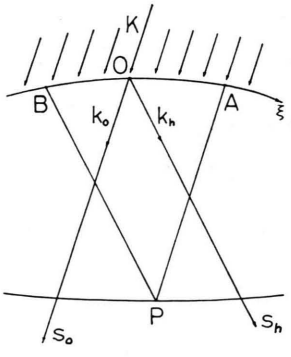

Fig. 1. The "inverted Borrmann triangle" PAB. Wave vectors $\boldsymbol{K}$, $\boldsymbol{k}_0$, $\boldsymbol{k}_h$ and coordinates s_0, s_h are also shown.

entrance surface which may be curved as shown in the Figure, ξ being the curved coordinate along the surface, $\gamma_0(\xi)$ the cosine of the angle between the surface normal and $\boldsymbol{k}_0$, and θ_B the Bragg angle. $v(s_0, s_h; s_0', s_h')$ in (7) and (8) is the Riemann function for a perfect crystal at (s_0', s_h') associated with the point (s_0, s_h) given by

$$v(s_0, s_h; s_0', s_h') = J_0(2\pi KC\sqrt{\chi_{-h}\chi_h(s_0 - s_0')(s_h - s_h')}), \tag{10}$$

where J_0 is the Bessel function of order 0. This has been shown by the present author and by Authier and Simon [5]. From (10) $\partial v/\partial s_h'$ is obtained as

$$\frac{\partial}{\partial s_h'} v(s_0, s_h; s_0', s_h') = F(2\pi KC\sqrt{\chi_{-h}\chi_h(s_0 - s_0')(s_h - s_h')}) \cdot \pi^2 KC\,\chi_{-h}\chi_h(s_0 - s_0'), \tag{11}$$

where

$$F(x) = J_1(x)/(x/2), \tag{12}$$

$J_1(x)$ being the Bessel function of order 1.

Equation similar to (6) and (7) can be obtained for ψ_h, namely

$$\frac{\partial^2\psi_h}{\partial s_0\,\partial s_h}(s_0, s_h) + \pi^2K^2C^2\chi_{-h}\chi_h\psi_h(s_0, s_h) = -i\pi KC\chi_h\frac{\partial}{\partial s_0}\exp(i2\pi\boldsymbol{h}\cdot\boldsymbol{u}(s_0, s_h))\psi_0(s_0, s_h) \tag{13}$$

and

$$\psi_h(s_0, s_h) = \psi_h^{(0)}(s_0, s_h) + \int\int \frac{\partial}{\partial s_0'}\exp(i2\pi\boldsymbol{h}\cdot\boldsymbol{u}(s_0', s_h')) \cdot [-i\pi KC\chi_h v(s_0, s_h; s_0', s_h')]\psi_0(s_0', s_h')\frac{dV'}{\sin 2\theta_B} \tag{14}$$

with

$$\psi_h^{(0)}(s_0, s_h) = \int [-i\pi KC\chi_h v(s_0, s_h; s_0', s_h')\,\Phi_0(s_0', s_h')]\frac{\gamma_0(\xi)}{\sin 2\theta_B}d\xi, \tag{15}$$

where $v(s_0, s_h; s_0', s_h')$ is also given by (10).

If wave functions

$$\varphi_0(s_0, s_h; s_0', s_h') \quad \text{and} \quad \varphi_h(s_0, s_h; s_0', s_h')$$

defined by

$$\varphi_0(s_0, s_h; s_0', s_h') = \delta(s_h - s_h') - F(2\pi KC\sqrt{\chi_{-h}\chi_h(s_0 - s_0')(s_h - s_h')}) \cdot \pi^2K^2C^2\chi_{-h}\chi_h(s_0 - s_0')/K\sin 2\theta_B \tag{16}$$

for $s_0 \geqq s_0'$ and $s_h \geqq s_h'$, and else zero, and by

$$\varphi_h(s_0, s_h; s_0', s_h') = -i\pi KC\chi_h J_0(2\pi KC\sqrt{\chi_{-h}\chi_h(s_0 - s_0')(s_h - s_h')})\,1/K\sin 2\theta_B \tag{17}$$

for $s_0 \geqq s_0'$ and $s_h \geqq s_h'$ and else zero are introduced, (7), (14), (8) and (15) can be written as

$$\psi_0(s_0, s_h) = \psi_0^{(0)}(s_0, s_h) + \iint_V P_{-h}(s_0', s_h')\,\varphi_{-h}(s_0, s_h; s_0', s_h')\,\psi_h(s_0', s_h')\,dV', \tag{18}$$

$$\psi_h(s_0, s_h) = \psi_h^{(0)}(s_0, s_h) + \iint_V P_h(s_0', s_h')\,\varphi_h(s_0, s_h; s_0', s_h')\,\psi_0(s_0', s_h')\,dV', \tag{19}$$

$$\varphi_0^{(0)}(s_0, s_h) = \int_B^A \varphi_0(s_0, s_h; s_0', s_h')\,\Phi_0(s_0', s_h')\,K\gamma_0(\xi)\,d\xi, \tag{20}$$

$$\psi_h^{(0)}(s_0, s_h) = \int_B^A \varphi_h(s_0, s_h; s_0', s_h')\,\Phi_0(s_0', s_h')\,K\gamma_0(\xi)\,d\xi, \tag{21}$$

where

$$P_{-h}(s_0', s_h') = K\frac{\partial}{\partial s_h'}\exp(-i2\pi h\,u(s_0', s_h')) = -i2\pi K\frac{\partial}{\partial s_h'}(\boldsymbol{h}\cdot\boldsymbol{u}(s_0', s_h'))\cdot\exp(-i2\pi\boldsymbol{h}\cdot\boldsymbol{u}(s_0', s_h')) \tag{22}$$

and

$$P_{\mathrm{h}}(s_0', s_{\mathrm{h}}') = K\frac{\partial}{\partial s_0'}\exp\left(i\,2\pi\boldsymbol{h}\cdot\boldsymbol{u}(s_0', s_{\mathrm{h}}')\right) = i\,2\pi K\frac{\partial}{\partial s_0'}\left(\boldsymbol{h}\cdot\boldsymbol{u}(s_0', s_{\mathrm{h}}')\right)\cdot\exp\left(i\,2\pi\boldsymbol{h}\cdot\boldsymbol{u}(s_0', s_{\mathrm{h}}')\right) \quad (23)$$

are probability amplitudes of scattering from the transmitted wave ($\boldsymbol{o}$-wave) to the diffracted wave ($\boldsymbol{h}$-wave) and from the $\boldsymbol{o}$-wave to the $\boldsymbol{h}$-wave, respectively.

The set of Eqs. (18) and (19) is not the solution to the Eqs. (6) and (13) or of the original equations (3), since the integrals include the wave functions ψ_0 and ψ_{h} themselves. It is a set of integral equations which is equivalent to the set of differential equations (3) and can be solved by successive approximation. The solutions are given by

$$\begin{aligned}\psi_0(s_0, s_{\mathrm{h}}) = \psi_0^{(0)}(s_0, s_{\mathrm{h}}) &+ \iint_V P_{-\mathrm{h}}(s_0', s_{\mathrm{h}}')\,\varphi_{-\mathrm{h}}(s_0, s_{\mathrm{h}}; s_0', s_{\mathrm{h}}')\,\psi_{\mathrm{h}}^{(0)}(s_0', s_{\mathrm{h}}')\,\mathrm{d}V' \\ &+ \iint_V\iint_V P_{-\mathrm{h}}(s_0', s_{\mathrm{h}}')\,\varphi_{-\mathrm{h}}(s_0, s_{\mathrm{h}}; s_0', s_{\mathrm{h}}')\,P_{\mathrm{h}}(s_0'', s_{\mathrm{h}}'')\,\varphi_{\mathrm{h}}(s_0', s_{\mathrm{h}}'; s_0'', s_{\mathrm{h}}'') \\ &\cdot\psi_0^{(0)}(s_0'', s_{\mathrm{h}}'')\,\mathrm{d}V'\,\mathrm{d}V'' + \cdots \end{aligned} \quad (24)$$

and by a similar expression for $\psi_{\mathrm{h}}(s_0, s_{\mathrm{h}})$, where $\psi_0^{(0)}$ and $\psi_{(0)}^0$ are given by (8) and (15), respectively.

Results and Discussion

The meaning of the integral equations (18) and (19) is as follows. $\psi_0^{(0)}(\boldsymbol{r})$ and $\psi_{\mathrm{h}}^{(0)}(\boldsymbol{r})$, given by (20) and (21), are the solutions for the perfect crystal to the Equations (3) by the method of Riemann [2]. For the $\boldsymbol{o}$-wave, the wave $\varphi_0(s_0, s_{\mathrm{h}}; s_0', s_{\mathrm{h}}')$ as given by (16) is generated at every point (s_0', s_{h}') on the entrance surface exposed to the incident wave, and for the $\boldsymbol{h}$-wave, $\varphi_{\mathrm{h}}(s_0, s_{\mathrm{h}}; s_0', s_{\mathrm{h}}')$ given by (17). All the effects of subsequent repeated Bragg reflections which the waves will suffer during their passage through the crystal are included in the functional form of φ_0 and φ_{h}. Thus when the entrance surface is plane and the incident wave is also plane, the integrals in (20) and (21) give the characteristic amplitude variation of transmitted and diffracted waves giving rise to equal-thickness fringes. This has been shown by Authier and Simon [5]. When the incident wave is very narrow so that $\Phi_0(r)$ in (20) and (21) can be approximated by the δ-function, the integrals in these equations give just $\varphi_0(s_0, s_{\mathrm{h}}; s_0', s_{\mathrm{h}}')$ and $\varphi_{\mathrm{h}}(s_0, s_{\mathrm{h}}; s_0', s_{\mathrm{h}}')$ themselves with appropriate constant factors. This result gives the same amplitude modulation as that of Kato's hyperbolic fringes in the case of spherical wave incidence, since this wave satisfies the Bragg condition only at points in a very narrow range on the surface, and outside this range the phase of Φ_0 oscillates so rapidly that it does not contribute appreciably to the integral. The value of

$$J_0\left(2\pi KC\sqrt{\chi_{-\mathrm{h}}\chi_{\mathrm{h}}(s_0 - s_0')(s_{\mathrm{h}} - s_{\mathrm{h}}')}\right),$$

the main factor of

$$\varphi_{\mathrm{h}}(s_0, s_{\mathrm{h}}; s_0', s_{\mathrm{h}}') \quad \text{and} \quad \varphi_{-\mathrm{h}}(s_0, s_{\mathrm{h}}; s_0', s_{\mathrm{h}}'),$$

is shown in Fig. 2, which also shows that the wave generated by scattering at a point $\mathrm{Q}(s_0', s_{\mathrm{h}}')$ spreads only inside the Borrmann triangle QCD (Figure 3). This is also the case for the wave $\varphi_0(s_0, s_{\mathrm{h}}; s_0', s_{\mathrm{h}}')$.

The double integrals in (18) and (19) represent the scattering from distorted parts of the crystal where $P_{-\mathrm{h}}$ and P_{h} given by (22) and (23) are ap-

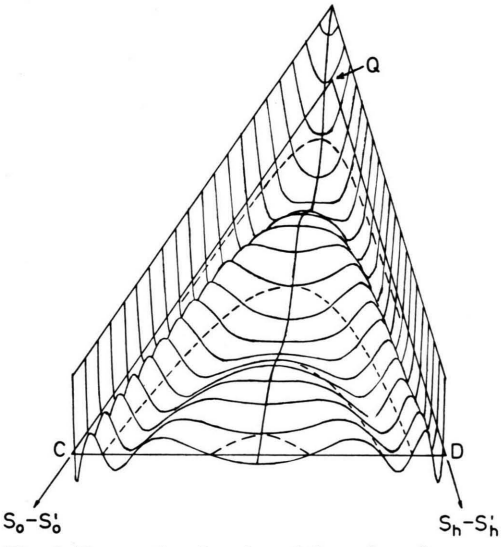

Fig. 2. Perspective drawing of the value of
$J_0(2\pi KC\sqrt{\chi_{-\mathrm{h}}\chi_{\mathrm{h}}(s_0' - s_0)(s_{\mathrm{h}} - s_{\mathrm{h}}')})$
showing the value of φ_{h} generated at $\mathrm{Q}(s_0', s_{\mathrm{h}}')$. Broken hyperbolae show the zero level.

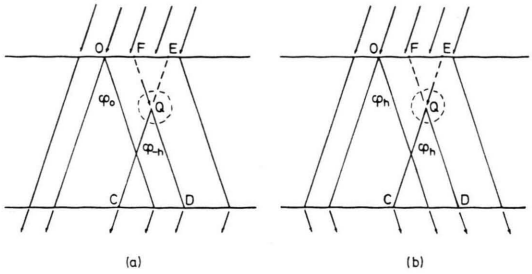

Fig. 3. Schematic illustration of the diffraction process inside a distorted crystal, (a) for the $\boldsymbol{o}$-wave and (b) for the $\boldsymbol{h}$-wave. The progression of waves generated at 0 on the entrance surface and at Q in the distorted region is shown.

preciable. The scattering at a single point $Q(s_0', s_h')$ from the $\boldsymbol{o}$-wave to the $\boldsymbol{h}$-wave is represented by the wave function $\varphi_h(s_0, s_h; s_0', s_h')$, its amplitude (including phase) being proportional to $P_h(s_0', s_h')$ and to $\psi_0(s_0', s_h')$, which is a resultant wave function of the $\boldsymbol{o}$-wave composed of $\psi_0^{(0)}$ generated at the surface and of $\boldsymbol{o}$-waves generated by scattering inside the inverted Borrmann triangle QEF (Figure 3). The scattered wave has an amplitude proportional to

$$2\pi K \frac{\partial}{\partial s_0'} (\boldsymbol{h} \cdot \boldsymbol{u})$$

and an additional phase factor $\exp(i 2\pi \boldsymbol{h} \cdot \boldsymbol{u})$ due to the displacement of atoms at and in the close vicinity of $Q(s_0', s_h')$.

As in the case of $\psi_h^{(0)}$, the effect of subsequent Bragg reflections is included in the form of $\varphi_h(s_0, s_h; s_0', s_h')$ shown in Figure 2.

A similar explanation holds for the scattering from the $\boldsymbol{h}$-wave to the $\boldsymbol{o}$-wave. The wave generated by scattering is $\varphi_{-h}(s_0, s_h; s_0', s_h')$, obtained by replacing $\boldsymbol{h}$ by $-\boldsymbol{h}$ in (17), the amplitude being proportional to

$$2\pi K \frac{\partial}{\partial s_h'} (\boldsymbol{h} \cdot \boldsymbol{u})$$

and having the additional phase factor

$$\exp(-i 2\pi \boldsymbol{h} \cdot \boldsymbol{u}).$$

Figures 3a and b depict schematically the diffraction process inside a distorted crystal, (a) for the $\boldsymbol{o}$-wave and (b) for the $\boldsymbol{h}$-wave. Each of the waves is composed of those generated at the surface and those from scattering in distorted regions. To avoid confusion only one wave is shown in each case. These generated waves proceed through the crystal with repeated Bragg reflections which are represented by the functions φ_0, φ_h and φ_{-h}.

For a precise numerical calculation the method of successive approximation has to be applied. The procedure is rather tedious unless the linear dimension of the distorted part is smaller than the extinction distance. It is not easy to say which of the two methods, the present one or the direct numerical integration of the original equations (3), is more convenient for the purpose. The present method is useful for the general understanding of the dynamical diffraction process inside distorted crystals and for getting characteristic features of the image in diffraction topographs of typical defects in crystals.

[1] S. Takagi, Acta Cryst. **15**, 1131 (1962).
[2] S. Takagi, J. Phys. Soc. Japan **26**, 1239 (1969).
[3] S. Takagi, Symposium, Recent Advances in the Experimental and Theoretical Methods of Crystal Structure Research. Munich, July 1962.
[4] F. Balibar and A. Authier, phys. stat. sol. **21**, 413 (1967).
[5] A. Authier and D. Simon, Acta Cryst. **A24**, 517 (1968).
[6] T. Katagawa and N. Kato, Acta Cryst. **A30**, 830 (1974).
[7] F. N. Chukhovskii and P. V. Petrashen, Acta Cryst. **A33**, 311 (1977).
[8] S. Takagi, Collected Abstracts, Tenth International Congress of Crystallography, Amsterdam, August 1975.
[9] S. Takagi, Collected Abstracts, Twelfth International Congress of Crystallography, Ottawa, August 1981.